DEPOSITION AND PROPERTY CHARACTERISATION OF TaN COATINGS DEPOSITED WITH DIFFERENT NITROGEN CONTENTS

✉ Gilberto Bejarano Gaitán[1]
Aida Milena Echavarría García[1]
Alix Caterine Quirama Ossa[1]
Jaime Alberto Osorio Vélez[2]

ABSTRACT

This study focused on the study of the influence of nitrogen content on the microstructure, chemical composition, mechanical and tribological properties of TaN coatings deposited on 420 stainless steel and silicon samples (100) using the magnetron sputtering technique. For the deposition of the TaN coatings an argon/nitrogen atmosphere was used, varying the nitrogen flux between 12% and 25%. For the coating characterization, scanning electron microscopy, energy-dispersive X-ray spectroscopy, atomic force microscopy, X-ray diffraction (XRD), micro-Raman spectroscopy, a micro-hardness tester, and a ball on disc tribometer were used. A refining of the columnar structure of the coatings, accompanied by a decrease in their thickness with the increased nitrogen content was observed. Initially, fcc-TaN (111) cubic phase growth was observed; this phase was changed to the fcc-TaN (200) above N_2 12%. For contents greater than N_2 18%, another nitrogen-rich phase was formed and the system tended towards amorphicity, particularly for a coating with N_2 25% content. The TaN-1sample deposited with N_2 12% in the gas mixture presented the highest micro-hardness value with 21.3GPa and the lowest friction coefficient and wear rate with 0.02 and 1.82x10^{-7} (mm^3/Nm), respectively. From the obtained results, an important relationship between the microstructural, mechanical and tribological properties of the coated samples and their nitrogen content was observed.

KEYWORDS: Hard coatings; Magnetron sputtering; Tantalum nitride; Surface modification; Wear resistance; Tribology.

DEPOSICIÓN Y CARACTERIZACIÓN DE LAS PROPIEDADES DE RECUBRIMIENTOS DE TaN DEPOSITADOS CON DIFERENTES CONTENIDOS DE NITRÓGENO

RESUMEN

Este trabajo se enfocó en el estudio de la influencia del contenido de nitrógeno sobre la microestructura, composición química, propiedades mecánicas y tribológicas de los recubrimientos de TaN depositados sobre acero inoxidable

1   Centro de Investigación, Innovación y Desarrollo de Materiales – CIDEMAT, Universidad de Antioquia-UdeA, Medellín – Colombia.

2   Grupo de Estado Sólido – Instituto de Física, Universidad de Antioquia-UdeA, Medellín – Colombia

✉ *Autor de correspondencia:* Bejarano-Gaitán, G. (Gilberto). Calle 60 75-150, Apto 821, Ribera del Valle, Medellín, Colombia / Tel.; (4)4462883
Correo electrónico: gilberto.bejarano@udea.edu.co

420 y silicio (100) mediante la pulverización catódica. Los recubrimientos se depositaron en una atmosfera de argón/ nitrógeno variando el flujo de nitrógeno entre 12% y 25%, y fueron caracterizados por SEM, EDX, DRX, AFM, Microraman, Microindentación y usando un tribómetro tipo bola sobre disco. Se apreció una refinación de la estructura columnar de los recubrimientos acompañado de una disminución de su espesor con el incremento del contenido de nitrógeno en éstos. Inicialmente se observó un crecimiento preferencial de la fase cúbica fcc del TaN (111), la cual cambió a la estructura fcc TaN (200) por encima del 12% de N_2. A contenidos mayores al 18% de N_2 se forman otras fases ricas en nitrógeno y el sistema tiende a la amorficidad, muy particularmente para un 25% de N_2. El recubrimiento TaN-1, depositado con 12% N_2 en la mezcla de gases, presentó la mayor dureza de 21.3 GPa, el menor coeficiente de fricción y tasa de desgaste de 0,02 y $1,82 \times 10^{-7}$ (mm^3/Nm), respectivamente. A partir de los resultados obtenidos se observó una importante relación entre la microestructura, las propiedades mecánicas y tribológicas de las muestras recubiertas y su contenido de nitrógeno.

PALABRAS CLAVE: recubrimientos duros; pulverización catódica; nitruro de Tantalio; modificación superficial; resistencia al desgaste; tribología.

DEPOSIÇÃO E CARACTERIZAÇÃO DAS PROPRIEDADES DE REVESTIMENTOS TaN DEPOSITADOS COM DIFERENTES CONTEÚDOS DE NITROGÊNIO

RESUMO

Este trabalho centrou-se em estudar a influência do conteúdo de nitrogênio sobre a microestrutura, composição química, propriedades mecânicas e tribológicas dos revestimentos TaN depositados em aço inoxidável 420 e de silício (100) por pulverização catódica. Os revestimentos foram depositados em uma atmosfera de árgon / nitrogênio variando o fluxo de nitrogênio entre 12% e 25%, e foram caracterizados por SEM, EDX, DRX, AFM, microraman, microindentation e usando um tribômetro do tipo bola no disco. Se apreciou um aperfeiçoamento da estrutura colunar dos revestimentos acompanhada por uma diminuição da sua espessura com o aumento do conteúdo de nitrogênio nestes. Inicialmente observou-se um crescimento preferencial da fase cúbica FCC TaN (111), que mudou a estrutura FCC TaN (200) acima de 12% de N_2. A conteúdos superiores a 18% de N_2 formam-se outras fases ricas em nitrogênio e o sistema tende a amorficidade, muito particularmente para um 25% de N_2. O revestimento de TaN-1, depositado com 12% N_2 na mistura de gás, presentou a maior dureza de 21,3 GPa, o menor coeficiente de fricção e taxa de desgaste de 0,02 e $1,82 \times 10^{-7}$ (mm^3/ Nm), respectivamente. A partir dos resultados observou-se relação importante entre a microestrutura, as propriedades mecânicas e tribológicas das amostras revestidas e o seu conteúdo de nitrogênio.

PALAVRAS-CHAVE: Revestimentos duros; Pulverização catódica; Nitreto de tântalo; Modificação da superfície; Resistência ao desgaste; Tribologia.

1. INTRODUCTION

The superficial modification of metallic materials with different coatings to improve their performance is one of the disciplines that are being investigated vertiginously. Tantalum nitride is a material characterized by high hardness, corrosion resistance, and chemical and thermal stability, which makes it very attractive for applications such as integrated circuits, diffusion barriers for copper-based metallization and resistors, as well as in the form of hard coatings for cutting and forming tools and machine parts (Riekkinen *et al.*, 2002; Bromark *et al.*, 1997).

However, other application fields are also promising for this material, such as bioengineering and materials science, which consider tantalum nitride biocompatible, whose features obtained from its manufacturing process can achieve porous structures (closed or interconnected), that can be favorably used in applications such as medical implants, where direct contact with bone structures is required, since its elastic modulus is very similar to such structures (Pino, 2008). The application field for tantalum nitride coatings is strongly linked to its microstructure, chemical composition, and mechanical and physicochemical properties, which in turn depend on, among other things, the nitrogen content and the Ta/N ratio of the coatings. In this study, the influence of nitrogen content on the microstructural and chemical properties, as well as on the mechanical and tribological behavior of the TaN coatings was determined. The obtained and discussed results represent an important database for future research and are helpful to determine the deposition process parameter of TaN coatings for an appropriate application. 420 stainless steel was chosen as the substrate because the future applications of this coated metal are directed towards surgical and dental instrumentation, which are usually manufactured with this steel. However, TaN coatings may be used in applications where high hardness and high wear and corrosion resistance are required, such as cutting and forming tools, extrusion dies, injection molds, discs and cutting blades, drills and end mills, among others. Single-crystal silicon substrates were used, as they are very suitable for spectroscopic and XRD characterization of the coatings, since the negative influence of the elements of steel is obviated.

2. EXPERIMENTAL DETAILS

2.1. Coatings Deposition

TaN coatings were developed using the unbalanced magnetron sputtering technique on Si (100) and 420 stainless steel substrates, which were grounded with silicon carbide abrasives with grit sizes of 350 to 1200, and finally polished with an alumina powder suspension to a mirror finish with an average roughness of Ra=0.05 μm, as measured with an optical profilometer. Thereafter, the samples were degreased in an ultrasonic bath with propanol and acetone and then dried using pressured air. Both propanol and acetone were used because when cleaning the samples only with propanol, they came out stained; this was avoided by adding the acetone. Before the deposition of the coatings, an ionic cleaning of the substrates and Ta target (99.9% high-purity) was carried out inside the vacuum chamber at a temperature of 100°C during a 15-minute period. After this, the TaN coatings were deposited varying the nitrogen gas flow between 8 and 20 sccm while the argon gas flow was maintained constant at 40 sccm, resulting in a chance of nitrogen gas flowing the $N_2/(Ar+N_2)$ gas mixture of between 12% and 25%, as indicated in **Table 1**. The gas flow was determined by a GFC17S mass flow controller from Aalborg. Other important process parameters were selected as follows: total time for each process: 4 hours; temperature: 120°C; Ta target power: 1,500W; bias voltage of substrates: (-50V); and process pressure: $6.3x10^{-3}$mbar. The samples were rotated at 20 rpm and located at a distance of 80 mm from the target. Before the deposition of each TaN coating system, a Ta interlayer with a thickness of about 100nm was deposited on the sample surfaces.
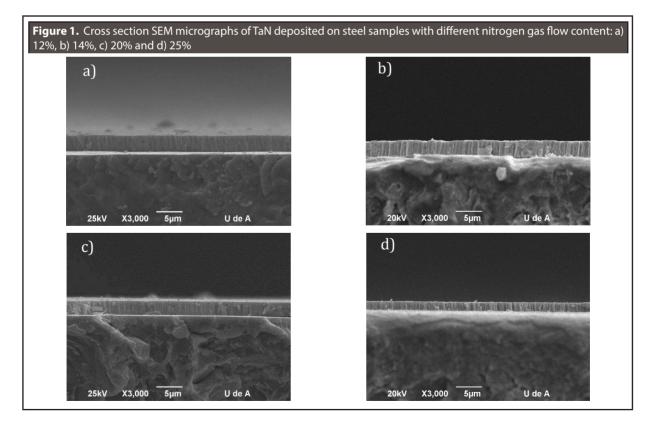
TABLE 1. NITROGEN CONTENTS IN THE GAS MIXTURES FOR THE DEPOSITED TaN COATINGS BY CONSTANT AR FLOW OF 40 SCCM

Sample	N2 gas flow (sccm)	$N_2/(Ar+N_2)$
TaN-1	8	12%
TaN- 2	10	14%
TaN- 3	13	18%
TaN- 4	15	20%
TaN- 5	20	25%

2.2. Coatings Characterization

The cross-section morphology and the thickness of the coatings, calculated as the average

of 3 measurements, were evaluated in a JEOL JSM-6490LV scanning electron microscope (SEM), while the chemical composition (weight % sigma between 1.06-1.18) was determined by energy-dispersive X-rayspectroscopy (EDX) and INCA energy software. The phases composition was characterized with a PANalytical Empyrean X-ray diffractometer using a Cu Kα1 radiation source, λ=1.540598 Å, 45kV, 40mA, an incidence angle of 1° and a step of 0.005 degrees per second. XRD patterns were analyzed with High Score Plus software and Rietveld refinement, so that the proportion of presented phases in the coating and crystallite size were calculated. Amorphous phases existing in the coatings were determined by a Horiba Jobin Yvon LabRAM high resolution micro-Raman using a helium-neon laser beam with a wavelength of 633nm and 17mW, and using data obtained from LabSpec software. The average surface roughness (Ra) of the coated samples, resulting from three measurements, was determined with an Easyscan 2 Flex atomic force microscope (AFM) sample stage in contact mode using a silicon nitride tip. The hardness of the uncoated and coated steel samples was determined by the Knoop test method. For the measurements, a Shimadzu HMV-G20 microindenter and a load of 25 grf were used according to the ASTM C1326 - 13norm. The hardness of each sample was calculated to the average value of 9 measurements. The friction coefficient and wear rate were evaluated in triplicate by a ball on disc tribometerusing a 6mm diameter alumina counter ball, 2mm radius wear track, sliding distance of 17.60 m and under 3N normal load, according to the ASTM G99-95 norm. The loss of mass during the test was determined by weighing the samples before and after the test with a precision balance Mattler Toledo UMX5 comparator, with a four-digit decimal. All experiments were conducted at a temperature of (19 ±2)°C and a relative humidity of (48.5 ±2)%. The samples for this study were previously washed in an ultrasonic bath with ethanol and then dried. The wear rate was determined by means of **Equation 1**.

Figure 1. Cross section SEM micrographs of TaN deposited on steel samples with different nitrogen gas flow content: a) 12%, b) 14%, c) 20% and d) 25%

$$K = \frac{M}{F.s} \qquad (1)$$

Where:

K is a wear rate (Kg/Nm)

M: mass lost in the trial (Kg)
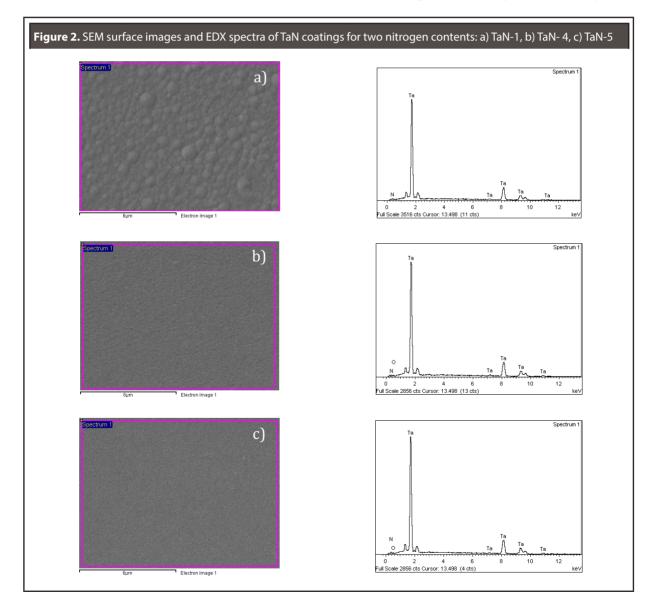
F: applied load (N)

s: sliding distance (m)

Additionally, the wear tracks were analyzed by the SEM, in order to elucidate the possible wear mechanisms.

3. RESULTS AND DISCUSSION

3.1. Coating Morphology and Chemical Composition

Figure 1 shows the cross-section SEM micrographs of TaN coatings for different nitrogen contents. These micrographs showed a homogenous microstructure for the coatings and a columnar grain growth perpendicular to the substrate's surface with possible nanoscale voids presented between the columns and at the grain boundaries following the Thornton growth model (Thornton, 1974).

Figure 2. SEM surface images and EDX spectra of TaN coatings for two nitrogen contents: a) TaN-1, b) TaN- 4, c) TaN-5

It was observed that the higher the nitrogen gas flow content, the more compact and defined the columns of the coatings were. In the same way, the coating thickness (measured in triplicate) decreases, as shown in **Table 2**. The elemental chemical composition of the TaN coatings, as determined by EDX, is shown in **Table 2**. The percentage content of the elements for each sample was the average of three measurements. Due to the low resolution of the ESD technique for determining the elemental chemical composition of elements such as N, C and B, among others, the atomic percentage of nitrogen in the coatings resulted from the difference between it and a Ta- content of 100%. Thus, the nitrogen content in the coatings increased slowly with the increment of N_2 gas flow in the Ar/N2 gas mixture, while the atomic percent of tantalum decreased. The thickness decrease is associated with the increase of nitrogen in the system gas mixture, which displaces the partial argon volume, decreasing the pulverization rate of Ta target as well as the deposition rate of the coatings on the substrate. Another reason for a decrease of the target sputtering rate is the formation of a compound layer on the Ta cathode (target poisoning). The low sputtering rate of the Ta target with higher nitrogen content, and therefore the reduction of deposition rate of TaN on the substrate, allows tantalum ions and atoms to better rearrange themselves on the substrate surface over time.
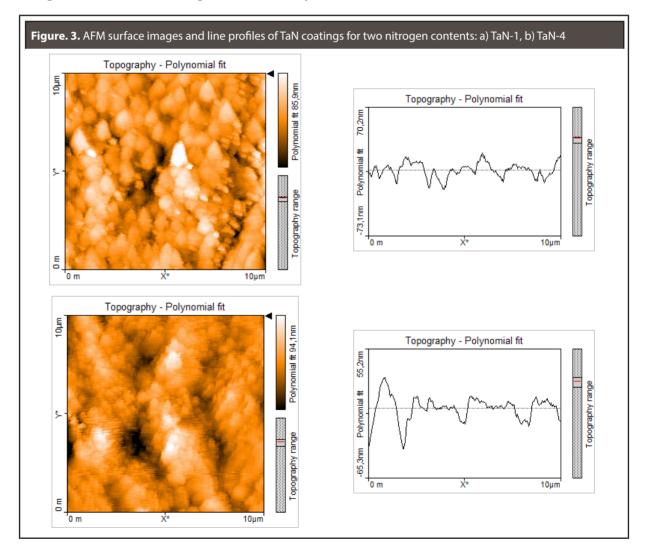

Figure. 3. AFM surface images and line profiles of TaN coatings for two nitrogen contents: a) TaN-1, b) TaN-4

TABLE 2. TaN COATINGS DEPOSITED ON SILICON SUBSTRATES: ATOMIC COMPOSITION, THICKNESS, ROUGHNESS, AND CRYSTALLITE SIZE

Sample	Composition (Atomic %)		Thickness (µm)	Roughness (nm)	Crystallite size (nm)
	Ta	**N**			
TaN- 1	53.7	46.3	3.3±0.06	9.4±1.12	8.6±0.013
TaN- 2	53.3	46.7	3.6±0.07	79.6±9.60	6.1±0.070
TaN- 3	49.6	50.4	2.2±0.04	12.7±1.52	1.9±0.024
TaN- 4	49.0	51.0	2.1±0.04	10.6±1.27	7.4±0.083
TaN- 5	47.7	52.3	1.8±0.36	35.0±4.20	12.5±0.014

This allows for greater grain stacking, increasing the coating density and decreasing its thickness. Moreover, by increasing the nitrogen content in the coatings, it continuously occupies the interstices of the TaN lattice, generating distortion of the lattice and leading to densification of the microstructure and probably to grain refinement. Similar features were observed by S. Tsukimoto *et al.* (Tsukimoto *et al.*, 2004) for the deposition and growth of TaN coatings.

The top SEM micrographs and resulting spectra of the chemical composition of the coated silicon samples TaN-2 and TaN-4 measured by EDX are shown in **Figure 2**. These micrographs show an apparent grain refinement when nitrogen content increases, according to the preceding discussion about **Figure 1**, where the grain boundaries practically disappear for nitrogen contents of 25%, also indicating an increase of the amorphicity degree of the coatings as will be discussed below. The grain size could not be measured because the AFM used did not have the necessary resolution and provided a lot of background noise.

In **Figure 3** the surface topographies of the coated samples TaN-1 and TaN-4 obtained by AFM are observed, including their respective linear profiles by means of which the average surface roughness value of 3 measurements was determined, as shown in **Table 2**. In both images, it can be seen that the grains consist of fine crystallites packaged in clusters
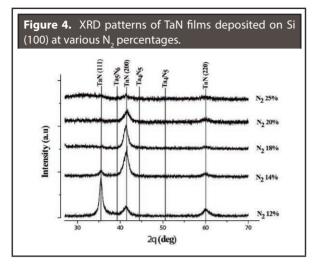
similar to a bunch of grapes. Such structures were also reported by Yang, J.J. *et al.* (Yang *et al.*, 2014).

Except for sample TaN-2, grown with N_2 14%, the remaining coatings had a similar roughness close to 10nm. However, the roughness increases again for nitrogen content of above 20%, which can be associated with the excessive amorphous phase formation of TaN identified in the XRD patterns and micro-Raman spectra, which will be discussed later. It is important to note that the roughness and preferential growth orientation of certain phases in the coatings deposited on silicon may vary if a substrate of 420 polycrystalline steel is used, due to the low roughness and mono-crystallinity of silicon.
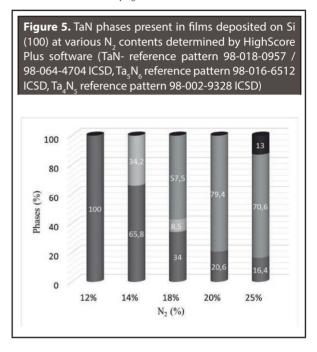
3.2. Composition of Coating Phases

XRD patterns of TaN coatings for different nitrogen content added to the N2/Ar gas mixture are shown in **Figure 4**. All coatings show characteristic peaks of cubic TaN, specifically fcc (111) (International Centre for Diffraction Data 1997), (200) (International Centre for Diffration Data 1997)and bcc (220) structures. The TaN (111) peak decreases when the nitrogen flux increases, and disappears almost completely above 14% N_2 content in the coating. Conversely, the cubic TaN peak (200) becomes more intense as the nitrogen content increases, but above 18% N_2, the peak decreases again and becomes wider. This behavior suggests a tendency towards structure amorphicity that is accompanied by the formation of the hexagonal phase Ta_5N_6 at 38° for samples coated with 14% and 18% N_2. Consequently, the sample coated with 25% N_2 presents a large amorphous zone between 30° and 35° and between 45° and 55°, where Ta_4N_5 and other nitrogen rich amorphous TaN phases appear, generating wide peaks in the TaN (220) cubic phase, and specifically in the TaN (200) phase. A possible explanation for the change in the orientation of TaN (111) to TaN (200) with the increase of nitrogen content is that the TaN (TaN-3 and TaN-4) phases are closer to Ta/N=1 stoichiometry, corresponding to the

most thermodynamically stable system and favoring the TaN (200) phase formation with the smallest growth energy (Moura *et al.*, 2011).

Figure 4. XRD patterns of TaN films deposited on Si (100) at various N_2 percentages.
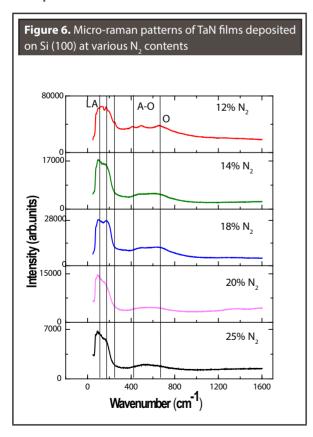
In order to identify and quantify the present phases in the different coatings of TaN, HighScore Plus software was used, performing Rietveld refinement in diffraction patterns. The resulting phases in each coating are shown in **Figure 5**, and a decrease of the cubic TaN can be seen as well as the beginning of the formation of the Ta_5N_6 and Ta_4N_5 phases, both with an amorphous character, when the nitrogen content increases. The Ta_4N_5 phase is significantly increased in the coatings with nitrogen percentages higher than 18%. Finally, in the TaN-5 coating, the high content of Ta_4N_5 and the appearance of the substoichiometric $Ta_{0.83}Na$ and $TaN_{0.9}$ phases suggest that this coating has an amorphous structure. Using Rietveld refinement, the crystallite size in TaN coatings for different nitrogen contents was determined. An example of two such calculations is shown here for a TaN-1 coating, which presents a crystallite with an 8.6 nm average size at its main peak localized at 35.48°, and for a TaN-4 coating with a crystallite size lower than 7.4 nm at its main peak localized at 41.24°. According to **Figure 5** the TaN-4 sample contents include 79.4% of the amorphous Ta_4N_5 phase, whose average crystallite size is 1.1nm, which leads to a reduced average crystallite size of this

coated sample compared to that of TaN-1. This is corroborated by the average peak full width at half maximum (FWHM) [°2θ] times 0.81: 1.59 for the TaN (200) phases in TaN-1 and TaN-4 respectively, and 3.91 for the Ta_4N_5 phase in the TaN-4 coating.

Figure 5. TaN phases present in films deposited on Si (100) at various N_2 contents determined by HighScore Plus software (TaN- reference pattern 98-018-0957 / 98-064-4704 ICSD, Ta_5N_6 reference pattern 98-016-6512 ICSD, Ta_4N_5 reference pattern 98-002-9328 ICSD)

It should be noted that the FWHM is inversely proportional to the crystallite size and is consistent with the previous analysis. To complement the XRD-evaluation of the existing phases in the coatings of TaN, and especially to support the possible existence of amorphous phases, a micro-Raman spectroscopy characterization was carried out on them. **Figure 6** shows the micro-Raman patterns obtained for TaN with different N_2 contents. The peak between 60 and 190 cm^{-1} is assigned to a longitudinal acoustic (LA) mode, while two wide peaks between 390 and 800 cm^{-1} are related to a first-order acoustic (A-O) and optical (O) mode, respectively. The latest is associated with the presence of point defects in the structure of TaN, indicating the presence of amorphous phases in the coatings. The small peak observed at 250 cm^{-1} for the TaN-1 sample is not reported in the literature when the stoichiometric value of nitrogen is less than 1.37 and is associated with an N-rich TaN phase (Spyropoulos-Antonakakis
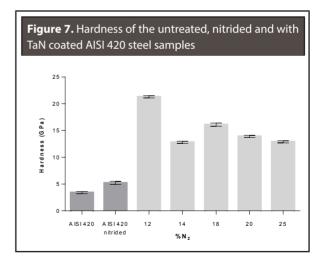
et al., 2013). With increasing nitrogen content the intensity of the peak between 390 and 800 cm^{-1} decreases, indicating a reduction in the coating's crystallinity. This behavior is related to an increase in the disorder of Ta- vacancies and N sites on sublattices, which leads further to a shift of the peak centered at 111.8 cm^{-1} towards lower wave length values for the TaN-4 and TaN-5 samples, indicating the occurrence of substoichiometric TaN- phases low in nitrogen. Similar results were obtained by (Spyropoulos-Antonakakis *et al.*, 2013; Lima *et al.*, 2012; Stoehr *et al.*, 2011). These observations are consistent with the results discussed regarding the above XRD measurements. These findings are also consistent with the results of H.B. Nie *et al.* (Nie *et al.*, 2001) who demonstrated through HRTEM analyses that the TaN coatings deposited by magnetron sputtering with high nitrogen contents present small crystalline domains embedded in an amorphous matrix.

Figure 6. Micro-raman patterns of TaN films deposited on Si (100) at various N$_2$ contents

3.3. Mechanical and Tribological Properties

3.3.1 Hardness

The hardness of the coated steel samples was determined by the Knoop indentation method, applying a low load of 250 mN to minimize the influence of the substrate on the coating's hardness. As shown in **Figure 7** the nitrided 420 steel sample exhibited a hardness of 5.2 GPa, which was higher than the hardness of the untreated sample at 3.4 GPa. In general terms, the hardness of the coated steel samples decreased with increasing N$_2$ contents in the coatings, this may be associated with, firstly, the effect of the hardness of the substrate since the thickness decreases with the nitrogen content, and on the other hand, with the increasing formation of nitrogen rich amorphous phases, as determined and described by the XRD and micro-Raman evaluation. The highest hardness, 21.3 GPa, was obtained for the TaN-1 sample, probably due to its high crystallinity and the elevated content of the cubic fcc phases. The relative low hardness of 12.8 GPa for the TaN-2 sample is possibly associated with the formation of the hexagonal Ta$_5$N$_6$ phase as addressed by **Figure 5**.

Figure 7. Hardness of the untreated, nitrided and with TaN coated AISI 420 steel samples
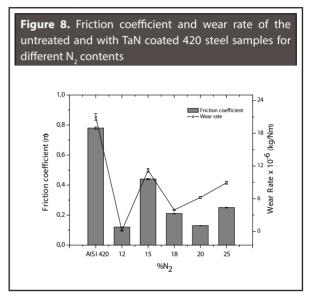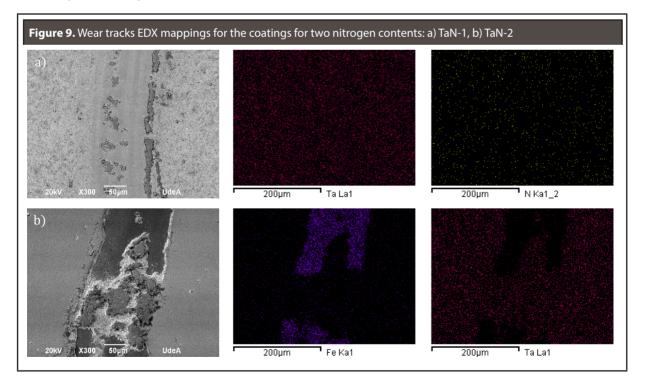
3.3.2 Wear Rate and Friction Coefficient

Figure 8 compares the friction coefficient and wear rate values of uncoated and TaN coated steel samples for different nitrogen gas flow contents in the

Ar/N_2- gas mixture. Of all the coated samples, TaN-1 presented the lowest wear rate due to its cubic fcc microstructure, and having the highest hardness and lowest friction coefficient. The TaN-2coating exhibited the highest wear rate, which is probably associated with its high content of the hexagonal phase Ta_5N_6 as well as with its high roughness, low hardness and high friction coefficient. The TaN-1 sample showed a wear coefficient 40 times lower than the uncoated 420 steel sample, indicating a promising application of TaN for wear protective coatings.

Wear tracks for TaN-1 and TaN-2 corresponding to the best and worst tribological behavior, respectively, are shown in **Figure 9**. In **Figure 9a**, the TaN-1 coating track shows an accumulation of material on the inner edge of the sliding track and some debris in the middle which were agglomerated and suffered plastic deformation in contact with the alumina counterbody. Regarding TaN-2 in **Figure 9b**, the coating has been removed entirely in some areas of the wear track, and several delamination sites can be found, which were evident on the inner and outer edges; this response seems to be correlated

with the highest roughness, coinciding with studies conducted by J. Takadoum and H. Houmid Bennani, who gave insights on the influence of thickness and roughness in coatings on tribological behavior (Takadoum & Bennani 1997). All coatings suffered adhesive wear mechanisms due to micro soldering at some points of contact as a result of relative movement generated in the test.

Figure 8. Friction coefficient and wear rate of the untreated and with TaN coated 420 steel samples for different N_2 contents

Figure 9. Wear tracks EDX mappings for the coatings for two nitrogen contents: a) TaN-1, b) TaN-2

4. CONCLUSIONS

The nitrogen content in the gas mixture study has a strong influence on the elemental chemical and phase composition, microstructure, and surface topography of the coatings, which this study was able to establish.

When the nitrogen content increases in the TaN coatings, it leads to a reduction of roughness, grain size, and coating thickness, which is probably associated with the process of nucleation and growth of the coating, the lattice distortion generated by the diffusion of nitrogen atoms to the interstices of the cubic TaN structure, and the reduction of the sputtering rate of the Ta-target, which has a primarily negative influence on the deposition rate of TaN on the substrates.

At a low nitrogen content, TaN possesses a crystalline cubic structure with preferential growth orientation in the (111) and (200) planes. This leads to a strong change to the (200) plane when accompanied by the formation of the hexagonal Ta_5N_6 phase for the TaN-2 and TaN-3 samples, simultaneously reducing coating hardness and wear resistance. When nitrogen contents are above 18% in the TaN- coatings, all peaks become wider and other nitrogen rich phases appear, suggesting a tendency towards structure amorphicity, as could be observed by the XRD and micro-Raman analyses. The obtained and discussed results of this study represent an important set of data for future research, and are helpful for selecting the appropriate parameter for the deposition process of TaN coatings for a given application.

ACKNOWLEDGMENTS

REFERENCES

International Center for Diffraction Data, (1997). JCPDS-Joint Committee on Powder Diffraction Standards - File card N°32-1283.

International Center for Diffration Data, (1997). JCPDS-Joint Committee on Powder Diffraction Standards - File card N°39-1485.

Lima, L.P.B.; Diniz, J.A.; Doi, I.; Miyoshi, J.; Silva, A.R.; Godoy Fo, J.; Radtke, C. (2012). Oxygen incorporation and dipole variation in tantalum nitride film used as metal-gate electrode. *Journal of Vacuum Science & Technology B: Microelectronics and Nanometer Structures*, 30(4), p.042202. [Online]. Available at: http://scitation.aip.org/content/avs/journal/jvstb/30/4/10.1116/1.4729599 [Consulted September 2, 2015].

Moura, C.; Constantin, D.G.; Munteanu, D. (2011). Structural , optical and decorative properties of TaNx thin films prepared by reactive magnetron sputtering. *Bulletin of the Transilvania University*, 4(2), pp. 59.

Nie, H.B.; Xu, S.Y.; Wang, S.J.; You, L.P.; Yang, Z.; Ong, C.K.; Li, J.; Liew, T.Y.F. (2001). Structural and electrical properties of tantalum nitride thin films fabricated by using reactive radio-frequency magnetron sputtering. *Applied Physics A Materials Science & Processing,* 73(2), pp. 229–236. [Online]. Available at: http://link.springer.com/10.1007/s003390000691.

Pino, J., (2008). Estudio nanométrico de biocompatibilidad y adhesividad celular a biomateriales utilizados en cirugía ortopédica. Santiago de Compostela.

Riekkinena, T.; Molariusa, J.; Laurilab, T.; Nurmelaa, A.; Sunia, I.; Kivilahtib, J.K. (2002). Reactive sputter deposition and properties of TaxN thin films. *Microelectronic Engineering*, 64(1-4), pp. 289–297.

Spyropoulos-Antonakakis, N.; Sarantopoulou, E.; Drazic, G.; Kollia, Z.; Christofilos, D.; Kourouklis, G.; Palles, D.; Cefalas, A.C. (2013). Charge transport mechanisms and memory effects in amorphous TaNx thin films. *Nanoscale research letters*, 8(1), p.432. [Online]. Available at: http://www.pubmedcentral.nih.gov/articlerender.fcgi?artid=4016540&tool=pmcentrez&rendertype=abstract.

Stoehr, M.; Shin, C.-S.; Petrov, I.; Greene, J. E. (2011). Raman scattering from TiNx (0.67 ≤ x ≤ 1.00) single crystals grown on MgO(001). *Journal of Applied Physics*, 110(8), pp. 0–4.

Takadoum, J.; Bennani, H.H., (1997). Influence of substrate roughness and coating thickness on adhesion, friction and wear of TiN films. *Surface and Coatings Technology*, 96, pp. 272–282.

Thornton, J.A., (1974). Influence of apparatus geometry and deposition conditions on the structure and topography of thick sputtered coatings. *Journal of vacumm science & Tecnologhy*, 11, pp. 666–670.

Tsukimoto, S.; Moriyama, M.; Murakami, M. (2004). Microstructure of amorphous tantalum nitride thin films. *Thin Solid Films*, 460(1-2), pp.222–226. [Online]. Available at: http://linkinghub.elsevier.com/retrieve/pii/S0040609004001257 [Consulted April 21, 2014].

Westergård, R.; Bromark, M.; Larsson, M.; Hedenqvist, P.; Hogmark, S. (1997). Mechanical and tribological characterization of DC magnetron sputtered tantalum nitride thin films. *Surface and Coatings Technology*, 97, pp. 779–784.

Yang, J.J.; Miao, F.M.; Tang, J.; Yang, Y.Y.; Liao, J.L.; Liu, N. (2014). Multi-scale kinetic surface roughening of reactive-sputtered TaN thin films characterized by wavelet transform approach. *Thin Solid Films*, 550, pp. 367–372. [Online]. Available at: http://linkinghub.elsevier.com/retrieve/pii/S004060901301804X [Consulted June 3, 2014].